Pseudogap effects induced by resonant pair scattering

Boldizsár Jankó, Jiri Maly, and K. Levin
The James Franck Institute, The University of Chicago, 5640 South Ellis Avenue, Chicago, Illinois 60637
(Received 15 May 1997)

We demonstrate how resonant pair scattering of correlated electrons above T_c can give rise to pseudogap behavior. This resonance in the scattering T matrix appears for superconducting interactions of intermediate strength, within the framework of a simple fermionic model. It is associated with a splitting of the single peak in the spectral function into a pair of peaks separated by an energy gap. Our physical picture is contrasted with that derived from other T-matrix schemes, with superconducting fluctuation effects, and with preformed pair (boson-fermion) models. Implications for photoemission and tunneling experiments in the cuprates are discussed. [S0163-1829(97)50742-9]

In recent years, pseudogap behavior of the underdoped cuprates has been observed in thermodynamic,[1] magnetic,[2] and angle-resolved photoemission spectroscopy (ARPES) data.[3] Of these three, ARPES experiments, which have established the presence of a Luttinger volume Fermi surface, place, perhaps, the most important constraints on any pseudogap scenario: they indicate that the pseudogap appears directly in the spectral function and its magnitude and symmetry[3] seem to evolve smoothly into that of the superconducting state. Furthermore, the minimum gap points in the pseudogap regime retrace the normal state Fermi surface.[4]

A variety of theoretical scenarios have been proposed for the origin of the pseudogap. Quantum Monte Carlo simulation studies have been carried out on both positive and negative U Hubbard models.[5] Alternative schemes relate the pseudogap to either magnetic pairing of spins,[6] resonating-valence bond (RVB) like pairing of chargeless spinons,[7] or precursor superconductivity effects.[8] The present paper addresses this last scenario, in part because of constraints from ARPES data and in part because the cuprates are short coherence length, quasi-two- dimensional superconductors, with anomalously low plasma frequencies.[8,9] They are, therefore, expected to exhibit important deviations from an abrupt, BCS-like transition.

In our physical picture, we associate an important component of the cuprate pseudogap with *resonant* scattering between electrons of opposite spin and small total momentum. This resonance arises in the presence of intermediate coupling and a sizable Fermi surface. A depression in the density of states occurs because states near this Fermi surface are unavailable for electrons in the Fermi sea to scatter into; such states are otherwise occupied by relatively long-lived (metastable) electron pairs. The related suppression in the spectral weight differs from that derived from conventional low-frequency and long-wavelength fluctuation effects.[10] In the present case it is the strength of the attractive interaction, rather than the critical slowing down (in proximity to T_c), which leads to the long-lived pair states. It should be noted that our resonant scattering approach is to be distinguished from previous precursor superconductivity models associated with either preformed pairs[11] or dynamic phase fluctuations.[8]

Our starting point is a scheme which connects the strong coupling, short coherence length description of superconductivity formulated by Leggett, Nozières and Schmitt-Rink, and Randeria and co-workers[12] with a well-established T-matrix formalism designed to treat normal state fluctuation effects in conventional superconductors.[10] We consider a generic model Hamiltonian

$$\mathcal{H}=\sum_{\mathbf{k}\sigma}\epsilon_{\mathbf{k}}c^{\dagger}_{\mathbf{k}\sigma}c_{\mathbf{k}\sigma}+\sum_{\mathbf{k}\mathbf{k}'\mathbf{q}}V_{\mathbf{k},\mathbf{k}'}c^{\dagger}_{\mathbf{k}+\mathbf{q}/2\uparrow}c^{\dagger}_{-\mathbf{k}+\mathbf{q}/2\downarrow}c_{-\mathbf{k}'+\mathbf{q}/2\downarrow}c_{\mathbf{k}'+\mathbf{q}/2\uparrow}, \quad (1)$$

where $c^{\dagger}_{\mathbf{k}\sigma}$ creates a particle in the momentum state $\mathbf{k}$ with spin σ, and $\epsilon_k=k^2/2m-\mu$ (we take $\hbar=k_B=1$). Here $V_{\mathbf{k},\mathbf{k}'}=g\varphi_{\mathbf{k}}\varphi_{\mathbf{k}'}$, $\varphi_{\mathbf{k}}=(1+k^2/k_0^2)^{-1/2}$, where for definiteness we take $k_0=k_F$; $g<0$ is the coupling strength. While we consider the s-wave symmetry case, d-wave symmetry can be readily introduced via $\varphi_{\mathbf{k}}\rightarrow(\cos k_x-\cos k_y)$. In the scheme of Nozières and Schmitt-Rink the transition temperature T_c must be obtained in combination with the chemical potential μ, by use of the Thouless criterion, $T^{-1}_{\mathbf{q}=\mathbf{0}}(\Omega=0)=0$ (see below), and the usual equation for particle number. When the parameter g is varied, the appropriate coupled equations lead to an interpolation scheme which contains the BCS limit for small g/g_c, where $\mu\approx E_F$, and that of Bose-Einstein condensation in strong coupling, where μ becomes negative. Here $g_c=-4\pi/mk_0$ is the value at which a bound state of the isolated pair first appears. *In order to capture the physics of the short coherence length regime, we chose g to be of the order* $g/g_c\approx 1$.[13]

In this paper, we provide a physical picture which associates this intermediate coupling regime with the onset of pair resonant scattering. Moreover, we extend the formulation of Ref. 12 so as to provide a basis for computing the spectral function and density of states and to simultaneously incorporate appropriate conservation laws.[14] To this end, we calculate the single-particle self-energy $\Sigma_{\mathbf{k}}(\omega)$, and the T matrix as shown diagrammatically in Fig. 1.[15] Analytically, the self-energy corresponds to

$$\Sigma_{\mathbf{k}}(i\zeta_l)=\frac{1}{\beta}\sum_{\mathbf{q},\Omega_n}\varphi^2_{\mathbf{k}-\mathbf{q}/2}T_{\mathbf{q}}(i\Omega_n)G^{(0)}_{\mathbf{q}-\mathbf{k}}(i\Omega_n-i\zeta_l), \quad (2)$$

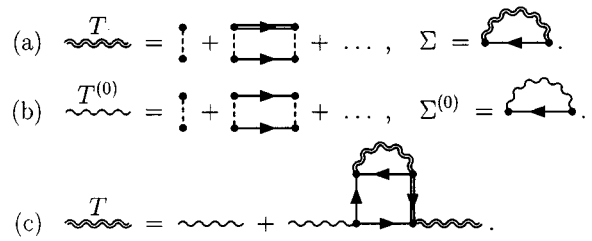

FIG. 1. Diagrams for coupled Σ, T, in full scheme (a) and lowest-order conserving scheme (b) used here. (c) represents a rewriting of T in (a).

and the T matrix, which may be written in the Dyson form shown in Fig. 1(c), is given by

$$T_{\mathbf{q}}(i\Omega_n)=\left[\frac{1}{g}+\frac{1}{\beta}\sum_{\mathbf{p},\zeta_l}\varphi_{\mathbf{p}}^2 G_{\mathbf{p}+\mathbf{q}/2}(i\zeta_l)G^{(0)}_{\mathbf{p}-\mathbf{q}/2}(i\Omega_n-i\zeta_l)\right]^{-1}. \tag{3}$$

Here $G_{\mathbf{k}}^{-1}(i\zeta_l)=G_{\mathbf{k}}^{(0)-1}(i\zeta_l)-\Sigma_{\mathbf{k}}(i\zeta_l)$ and $G_{\mathbf{k}}^{(0)}(i\zeta_l)=(i\zeta_l-\epsilon_k)^{-1}$. Finally, the spectral function is defined as $A_{\mathbf{k}}(\omega)=-\pi^{-1}\mathrm{Im}[G_{\mathbf{k}}(i\zeta_l\rightarrow\omega+i0)]$; this leads to the density of states, $N(\omega)=\Sigma_{\mathbf{k}}A_{\mathbf{k}}(\omega)$.

The choice of diagrams to include in a T-matrix scheme has been extensively discussed in the literature.[15–17] Our asymmetric choice [Fig. 1(a)]—in which the T matrix contains one self-energy renormalized and one ''bare'' propagator—builds on the early work of Kadanoff and Martin.[16] When this diagrammatic scheme was applied to conventional superconducting fluctuation effects it was shown[15] that the fluctuation gap above T_c smoothly evolved into the superconducting gap below T_c. Moreover, this approach is known[15,16] to reproduce the conventional BCS theory in the appropriate weak coupling limit. Direct connection can be made to the related theories of Marcelja[18] and Yamada and collaborators[19] if the full line in the ''box'' (the pair fluctuation self-energy) of Fig. 1(c) is replaced by a noninteracting line. Finally, it is straightforward to demonstrate using the more general criteria introduced by Kadanoff and Baym[20] that this theory preserves all conservation laws.

It has been shown that the results of the full ''mode-coupling'' scheme of Fig. 1(a) are qualitatively captured by the lowest order conserving approximation of Fig. 1(b);[18] this approximation, nevertheless, goes beyond the original work of Nozières and Schmitt-Rink. Unlike other T-matrix approaches, where higher-order self-consistency effects tend to diminish leading order features,[21] it is found[18] that within the present framework the inclusion of ''mode-coupling'' effects amplify these first-order (pseudogap) features. For simplicity, we, therefore, focus on the lowest-order approximation. The discussion of feedback effects is deferred to a future publication.

In our scenario the physical process which generates the pseudogap is resonant pair scattering (above T_c), arising from the condition that the real part of the inverse T matrix, $\mathrm{Re}[T_{\mathbf{q}}^{-1}(\Omega=\Omega_{\mathbf{q}})]=0$, when the imaginary part, $\mathrm{Im}[T_{\mathbf{q}}^{-1}(\Omega_{\mathbf{q}})]$, is sufficiently small. This resonant behavior is manifested as a sharp peak in $\mathrm{Im}[T_{\mathbf{q}}(\Omega)]$. This peak is in turn reflected in the electronic self-energy and the spectral

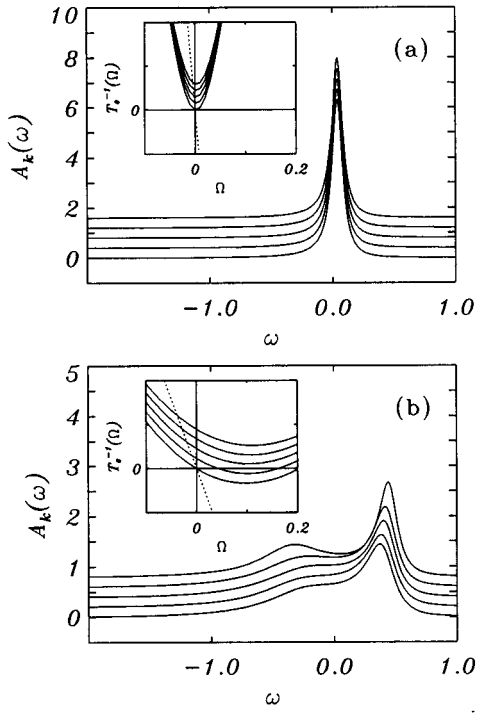

FIG. 2. $A_{\mathbf{k}}(\omega)$ vs ω for weak ($g/g_c=0.6$) in (a) and intermediate ($g/g_c=1.0$) coupling in (b). T/T_c varies from 1.0 to 1.1. Insets plot $\mathrm{Re}[T^{-1}_{\mathbf{q}=\mathbf{0}}(\Omega)]$ (solid lines, for same T/T_c, as in main figure), and $-\mathrm{Im}[T^{-1}_{\mathbf{q}=\mathbf{0}}(\Omega)]^{-1}$ (dashed lines, at $T=T_c$).

function. The pair resonance condition is illustrated in the insets of Fig. 2, where the behavior of $\mathrm{Re}[T^{-1}_{\mathbf{q}=\mathbf{0}}(\Omega)]$, as a function of frequency, is contrasted for weak ($g/g_c<1$) [Fig. 2(a)] and intermediate ($g/g_c\approx 1$) [Fig. 2(b)] couplings. Each series of curves corresponds to varying temperature. The dashed lines indicate the form of $\mathrm{Im}[T_{\mathbf{q}}^{-1}(\Omega)]$ at T_c in each of the two cases. The critical value g_c establishes the approximate dividing point between resonant and nonresonant scattering. As can be seen, there is a finite frequency zero crossing of $\mathrm{Re}[T_{\mathbf{q}}^{-1}(\Omega)]$ for $T>T_c$, corresponding to resonant scattering, in the stronger coupling limit. The resonance energy increases as a function of temperature T and $\mathbf{q}$ until it disappears at a crossover wave vector $\mathbf{q}^*$ or temperature T^*.

The associated spectral functions $A_{\mathbf{k}}(\omega)$ for each of the two cases considered in the insets are numerically computed from the self-energy using Eq. (2) and plotted for the case $k=k_F$ in the main portion of Fig. 2 as a function of ω, for varying T. (Throughout, the unit of energy is E_F.) Although the numerical integrations involved are computationally intensive, the integrated spectral weight is unity to several significant digits for each spectral curve presented. In the stronger coupling limit and at sufficiently low T [Fig. 2(b)], the two-peaked structure characteristic of a pseudogap appears and becomes more pronounced with larger g/g_c. In the more weakly coupled limit ($g/g_c=0.6$), the single-peak behavior characteristic of a normal Fermi liquid is recovered, as shown in Fig. 2(a). In general, the two-peaked structure correlates with the presence of a resonance in the T matrix. For g slightly greater than g_c, the two maxima are resolvable up to T^* of the order of several T_c.

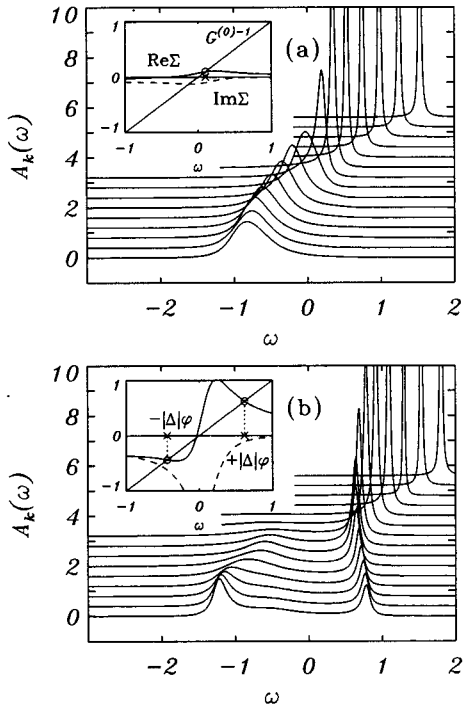

FIG. 3. $A_{\mathbf{k}}(\omega)$ vs ω for (a) weak ($g=0.8g_c$) and (b) intermediate ($g=1.2g_c$) coupling, from $k<k_F$ (bottom curve) to $k>k_F$ (top curve). Note signatures in (b) of ''particle-hole mixing.'' In the insets are plotted the corresponding $\mathrm{Im}[\Sigma_{\mathbf{k}}(\omega)]$ and $\mathrm{Re}[\Sigma_{\mathbf{k}}(\omega)]$ for $k=k_F$ and T slightly above T_c.

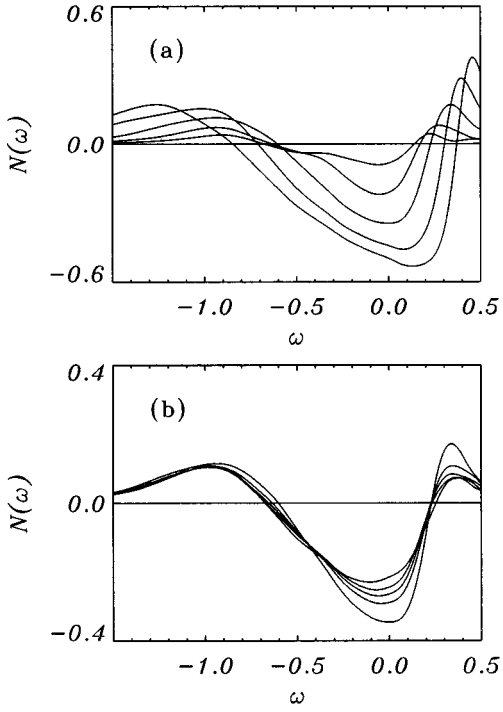

FIG. 4. $N(\omega)$ vs ω for $g/g_c=0.8$ to 1.1 and $T=T_c$ (a), and for $T/T_c=1.0$ to 1.2, at $g=g_c$, (b). The normal-state density of states is subtracted off in both cases (see text).

An intuitive understanding of the splitting of the spectral peak into a pair of asymmetrically broadened peaks may be gained by examining the imaginary part of the self-energy. On the real frequency axis ($i\zeta_l\rightarrow\omega+i\delta$), $\mathrm{Im}[\Sigma_{\mathbf{k}}(\omega)]$ is given by

$$\mathrm{Im}[\Sigma_{\mathbf{k}}(\omega)]=-\sum_{\mathbf{q}}\varphi^2_{\mathbf{k}-\mathbf{q}/2}\mathrm{Im}[T_{\mathbf{q}}(\omega+\epsilon_{\mathbf{q}-\mathbf{k}})]\times[f(\epsilon_{\mathbf{q}-\mathbf{k}})+n(\omega+\epsilon_{\mathbf{q}-\mathbf{k}})], \quad (4)$$

where $f(x),n(x)=(e^{\beta x}\pm 1)^{-1}$.[22] For intermediate coupling strengths, a resonance condition leads to a peak in $\mathrm{Im}[T_{\mathbf{q}}(\Omega)]$ at small frequencies and momenta, which in turn yields a maximum in $-\mathrm{Im}[\Sigma_{\mathbf{k}}(\omega)]$ at $\omega+\epsilon_{\mathbf{k}}\approx 0$ [see the inset of Fig. 3(b)]. The frequency weight under this peak is written as $\pi|\Delta|^2\varphi^2_{\mathbf{k}}$, where $|\Delta|$ can be viewed as the pseudogap energy. This peak in $-\mathrm{Im}[\Sigma_{\mathbf{k}}(\omega)]$ implies—via the Kramers-Krönig relation—a corresponding resonance structure in $\mathrm{Re}[\Sigma_{\mathbf{k}}(\omega)]$ at the same frequency $\omega\approx-\epsilon_{\mathbf{k}}$. In this way $A_{\mathbf{k}}(\omega)$ acquires two peaks separated by $2|\Delta|\varphi_{\mathbf{k}}$ with

$$|\Delta|^2\approx\sum_{\mathbf{q}}\int_{-\infty}^{+\infty}\frac{d\Omega}{\pi}n(\Omega)\mathrm{Im}[T_{\mathbf{q}}(\Omega)]. \quad (5)$$

The asymmetric broadening[22] of the two spectral peaks is a generic feature of our results and is due to the interaction of correlated pairs with the Fermi sea. This asymmetry, which is contained in Eq. (4), reflects that in $\mathrm{Im}[T_{\mathbf{q}}(\Omega)]$, as a function of Ω. In Fig. 3 we plot the momentum dependence of the spectral function slightly above T_c for weak [Fig. 3(a)] and intermediate [Fig. 3(b)] coupling, along with typical self-energies shown in the insets. The former case shows the single-peak structure which evolves with $\mathbf{k}$ in a fashion characteristic of a finite temperature Fermi liquid.[22] In the stronger coupling limit [Fig. 3(b)] the spectral weight shifts from the negative to the positive frequency peak as the momentum vector $\mathbf{k}$ passes through the Fermi surface. Close to the Fermi momentum the peaks disperse roughly as $E_{\mathbf{k}}=\pm\sqrt{\epsilon^2_{\mathbf{k}}+|\Delta|^2\varphi^2_{\mathbf{k}}}$. This dispersion provides a predictive signature for future ARPES measurements, within the precursor superconductivity scenario. Indeed, this behavior is reminiscent of the particle-hole mixing found in photoemission measurements on the superconducting state.[23,24]

Finally, the density of states $N(\omega)$ is plotted in Fig. 4 as a function of energy. This quantity may be directly related to tunneling as well as to thermodynamic measurements in the pseudogap regime. The asymmetry in the curves reflects, in part, the asymmetry of the spectral functions seen in Figs. 2 and 3. For clarity the results are represented by subtracting the ''normal'' state curve, obtained, for definiteness, in the very weak coupling limit. Figure 4(a) indicates the coupling constant dependence of $N(\omega)$ and Fig. 4(b) the corresponding temperature dependence for fixed g. A depression in $N(\omega)$—which increases with g—develops at smaller couplings, and persists to higher temperatures, than do pseudogap effects in the spectral function (see Fig. 3).

In summary, we have demonstrated how resonant pair scattering above T_c gives rise to a splitting of the spectral function $A_{\mathbf{k}}(\omega)$, as well as a density-of-states depression. Experimental observation of the former is the more significant manifestation of pseudogap behavior, providing strong

constraints on theoretical models. Our precursor superconductivity scenario has predictive signatures: an asymmetry in the widths of the two spectral peaks and a **k**-dependent dispersion of the $T>T_c$ spectral function, qualitatively similar to that of the BCS state. A $d_{x^2-y^2}$ symmetry of the normal state gap will arise naturally in the present scenario, for a d-wave superconducting instability. This would be accompanied by a spectral peak broadening proportional to $(\cos k_x - \cos k_y)^2$. The present picture should be differentiated from preformed pair models: the correlated pairs of our picture have significant spatial extent and fail to obey Bose statistics. Furthermore, in contrast to the stripe picture of Emery and Kivelson, the amplitude and phase of this paired state is never established beyond the dimensions and lifetime of a single pair. *Quasi-two-dimensionality as well as reduced electronic screening*[9] *will enhance our pseudogap effects, which should, then, become more pronounced as the insulator is approached.* Magnetic correlations may, also, ultimately play a role in the extreme underdoped regime. Nevertheless, short coherence lengths and quasi-2D features suggest that precursor superconductivity is present to some degree and must necessarily be calibrated in order to obtain a full understanding of the cuprate pseudogap.

We would like to thank J. C. Campuzano, H. Ding, L. P. Kadanoff, A. Klein, I. Kosztin, P. C. Martin, M. Norman, B. R. Patton, and especially Y. M. Vilk for useful discussions. This research was supported in part by the Natural Sciences and Engineering Research Council of Canada (J.M.) and the Science and Technology Center for Superconductivity funded by the National Science Foundation under award No. DMR 91-20000.

[1] J. W. Loram and J. R. Cooper, J. Phys. I **6**, 2237 (1996).

[2] C. P. Slichter, in *Strongly Correlated Materials*, edited by K. Bedell *et al.* (Addison-Wesley, Reading, MA, 1994), p. 427.

[3] A. G. Loeser *et al.*, Science **273**, 325 (1996); H. Ding *et al.* Nature (London) **382**, 51 (1996).

[4] H. Ding *et al.* Phys. Rev. Lett. **78**, 2628 (1997).

[5] M. Ulmke *et al.*, Phys. Rev. B **54**, 16 523 (1996); M. Randeria *et al.*, Phys. Rev. Lett. **69**, 2001 (1992).

[6] A. V. Chubukov *et al.*, J. Phys. Condens. Matter **8**, 10 017 (1996); J. R. Schrieffer and A. P. Kampf, J. Phys. Chem. Solids **56**, 1673 (1995).

[7] P. W. Anderson, *The Theory of Superconductivity in the High-T_c Cuprate Superconductors* (Princeton University Press, Princeton, 1997). See also Ref. 24, below.

[8] V. J. Emery and S. A. Kivelson, Nature (London) **374**, 434 (1995); Phys. Rev. Lett. **74**, 3253 (1995); V. J. Emery *et al.*, Phys. Rev. B **57**, 6120 (1997).

[9] J. Maly *et al.*, Phys. Rev. B **54**, 15 657 (1996).

[10] B. R. Patton, Phys. Rev. Lett. **27**, 1273 (1971).

[11] J. Ranninger and J. M. Robin, Phys. Rev. B **53**, R11 961 (1996); V. B. Geshkenbein *et al.*, *ibid.* **55**, 3173 (1997); A. S. Blaer *et al.*, *ibid.* **55**, 6035 (1997).

[12] A. J. Leggett, J. Phys. (Paris) **41**, C7 (1980); P. Nozières and S. Schmitt-Rink, J. Low Temp. Phys. **59**, 195 (1985); M. Randeria *et al.*, Phys. Rev. Lett. **62**, 981 (1989).

[13] F. Pistolesi and G. Strinati, Phys. Rev. B **49**, 6356 (1994).

[14] J. W. Serene, Phys. Rev. B **40**, 10 873 (1989).

[15] B. R. Patton, Ph.D. thesis, Cornell University, 1971.

[16] L. P. Kadanoff and P. C. Martin, Phys. Rev. **124**, 670 (1961). See also A. Klein, Nuovo Cimento **25**, 788 (1962).

[17] R. Micnas *et al.*, Phys. Rev. B **52**, 16 223 (1995); R. Haussmann, *ibid.* **49**, 12 975 (1994).

[18] S. Marcelja, Phys. Rev. B **1**, 2531 (1970).

[19] A. Tokimitu *et al.*, J. Phys. Soc. Jpn. **60**, 380 (1991).

[20] L. P. Kadanoff and G. Baym, Phys. Rev. **124**, 287 (1961).

[21] J. M. Vilk and A.-M. S. Tremblay [cond-mat/9702188 (unpublished)] recently concluded that renormalizing both Green's functions in the spin susceptibility also leads to inconsistencies in the magnetic case.

[22] During numerical evaluations we neglect the $f(\epsilon_{\mathbf{q}-\mathbf{k}})$ in this equation, since it is insignificant in generating the pseudogap. However, this approximation overestimates the particle-hole asymmetry in spectral properties. Small variations in μ with T were also neglected to avoid numerical complexity.

[23] J. C. Campuzano *et al.*, Phys. Rev. B **53**, R14 737 (1996).

[24] Similar theoretical results have been reported by P. A. Lee *et al.*, cond-mat/9701168 (unpublished).